Supporting Information

Multi-shelled hollow layered double hydroxides with enhanced performance for oxygen evolution reaction

Yongji Qin,*[a] Bingqing Wang,[b] Yuan Qiu,[a] Xijun Liu,[a] Gaocan Qi,[c] Shusheng Zhang,[d] Aijuan Han,*[b] Jun Luo [a] and Junfeng Liu [b]

a. Institute for New Energy Materials & Low-Carbon Technologies and Tianjin Key Lab for Photoelectric Materials & Devices, School of Materials Science and Engineering, Tianjin University of Technology, Tianjin 300384, China. E-mail: 383151026@qq.com (Y. Qin).

b. State Key Laboratory of Chemical Resource Engineering, Beijing University of Chemical Technology, Beijing 100029, China. E-mail: hanaijuan@mail.buct.edu.cn (A. Han).

c. Tianjin Key Lab for Photoelectric Materials & Devices, School of Materials Science and Engineering, Tianjin University of Technology, Tianjin 300384, China.

d. College of Chemistry, Zhengzhou University, Zhengzhou 450000, China

Experimental Section

1.1 Chemicals: Commercial chemicals were bought from Sigma-Aldrich (ACS grade) and used as received except otherwise noted.

1.2 Synthesis of multi-layered (ZIF-67@ZIF-8)$_n$: In a typical procedure, to prepare the ZIF-67 crystal, 5 mL of 2 M cobalt nitrate hexahydrate and 100 mL of 4 M 2-methylimidazole (2-MIM) in methanol solution were firstly prepared by mixing under magnetic stirring for 1 hour, and then left undisturbed for 24 h. The purple precipitate was centrifuged, washed with solvent three times and re-dispersed in 30 mL of methanol (suspension I).

To prepare ZIF-67@ZIF-8, suspension I was mixed with 30 mL of 0.27 M 2-MIM methanol solution and stirred for 10 min. Then, 5 mL of 0.4 M zinc nitrate hexahydrate methanol solution was added. After another 10 minutes stirring, the mixture was left undisturbed for 1 h. The precipitate was centrifuged, washed with solvent three times. Finally, the products were re-dispersed in 30 mL of methanol (suspension II).

To prepare (ZIF-67@ZIF-8)$_2$, at first, 20 mL of suspension II was mixed with 30 mL of 0.27 M 2-MIM methanol solution and stirred for 10 min. Then, 5 mL of 0.4 M cobalt nitrate hexahydrate methanol solution was added. After another 10 minutes stirring, the mixture was left undisturbed for 1 h. The precipitate was centrifuged, washed with solvent three times and re-dispersed in 20 mL of methanol (suspension III). Then, the suspension III was mixed with 30 mL of 0.27 M 2-MIM methanol solution and stirred for 10 min. Then, 5 mL of 0.4 M zinc nitrate hexahydrate methanol solution was added. After another 10 minutes stirring, the mixture was left undisturbed for 1 h. The precipitate was centrifuged, washed with solvent three times and re-dispersed in 20 mL of methanol (suspension IV).

To prepare (ZIF-67@ZIF-8)$_3$, the procedure was similar to that of (ZIF-67@ZIF-8)$_2$, except using 10 mL of suspension IV as the seed for repeat growth of ZIF-67 and ZIF-8. Finally, the products were dispersed in 10 mL of methanol for further use (suspension V).

1.3 Synthesis of multi-shelled hollow LDHs (MSH-LDHs): To prepare single-shelled hollow LDHs (SSH-LDH), typically, 5 mL of suspension II (ZIF-67@ZIF-8) was washed and redispersed in 5 mL ethanol. Then, the resultant solution was poured into a mixed solution (33 mL EtOH, 2 mL MeOH) containing 0.01 M $Ni(NO_3)_2 \cdot 6H_2O$ and 0.001 M $Fe(NO_3)_3 \cdot 9H_2O$. The mixture was aged at room temperature for 1 h. After the purple color disappeared, a yellow product was centrifuged, washed with ethanol and dried in a vacuum oven at 70 °C.

The synthesis procedure of double-shelled hollow LDHs (DSH-LDH) and triple-shelled hollow LDHs (TSH-LDH) was similar to that of SSH-LDH, except 5 mL of suspension IV and V instead of suspension II were used as precursors, respectively. The concentration of $Ni(NO_3)_2 \cdot 6H_2O$ and $Fe(NO_3)_3 \cdot 9H_2O$ was doubled or tripled for synthesizing DSH-LDH and TSH-LDH, respectively, compared to that was used for SSH-LDH.

1.4 Characterization: The morphologies and sizes of samples were characterized by a transmission electron microscope (TEM, Hitachi HT-7700) operated at 100 kV. The energy-dispersive X-ray spectroscopy (EDX) and elemental mapping connected to the high-resolution TEM was performed by a field emission electron microscope (JEM-2100F) operated at 200 kV. Powder X-ray diffraction (XRD) was tested on a Shimadzu XRD-6000 diffractometer with Cu Kα radiation (λ=1.5418 Å). The X-ray photoelectron spectroscopy (XPS) was accomplished on a Thermo ESCALAB 250Xi system with an Al Kα X-ray source. The N_2 adsorption–desorption isotherms and surface areas were determined using an Quantachrome Autosorb-iQ surface area analyzer. The samples were degassed at 423 K for 12 h prior to analysis. The Brunauer Emmett Teller (BET) method was used to calculate the specific surface areas. The pore size distributions were calculated from the Barrett-Joyner-Halenda (BJH) desorption method.

1.5 OER test: A CHI 660D (Chenhua, Shanghai) workstation was used to test all the electrochemical measurements, using a typical three-electrode system at RT with carbon rod as counter electrode as well as Hg/HgO electrode as reference electrode. All the inks were made by mixing 5 mg samples with 50 μL of 0.5% Nafion solution and 950 μL ethanol. After 1 h sonication, the ink was dried onto the carbon paper to make a 1 mg cm^{-2} loading. The OER results were obtained in 1 M KOH aqueous solution and then transformed to reversible hydrogen electrode (RHE) potentials with iR calibration. Electrochemical impedance spectroscopy (EIS) was performed at overpotential from 100000 to 10^{-1} Hz with a 5 mV voltage range. The stability was tested at constant overpotentials for ~60 h.

Figures

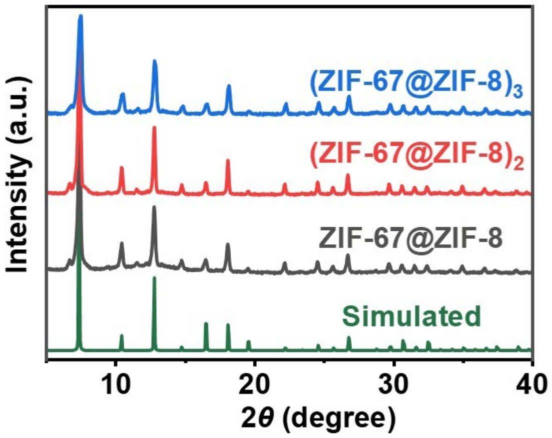

Fig. S1 XRD patterns of ZIF-67@ZIF-8, (ZIF-67@ZIF-8)$_2$ and (ZIF-67@ZIF-8)$_3$.

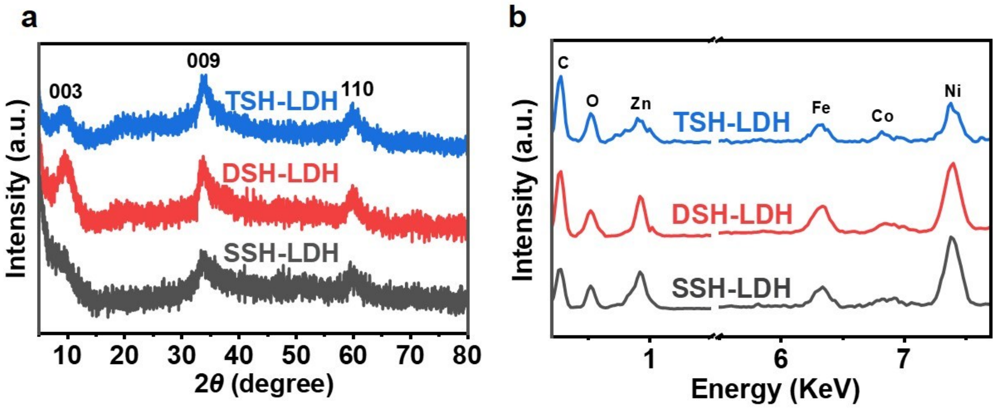

Fig. S2 (a) XRD patterns and (b) EDX spectra of SSH-LDH, DSH-LDH, and TSH-LDH.

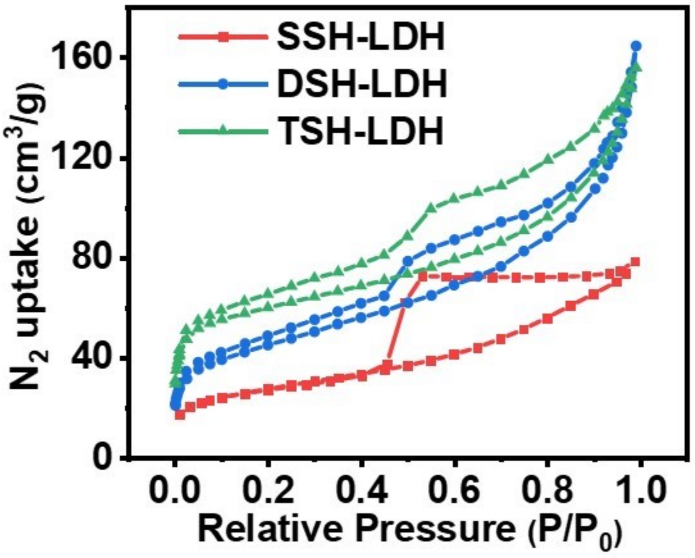

Fig. S3 N_2 adsorption-desorption isotherms of SSH-LDH, DSH-LDH and TSH-LDH.

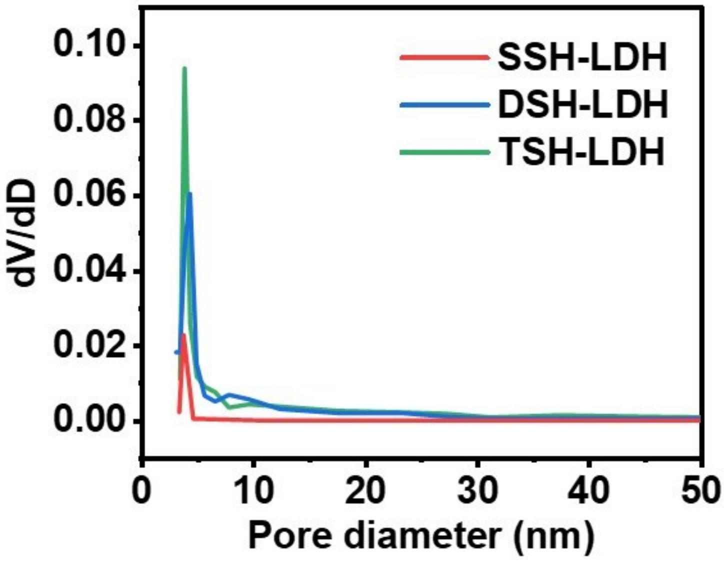

Fig. S4 The BJH pore size distributions of SSH-LDH, DSH-LDH and TSH-LDH.

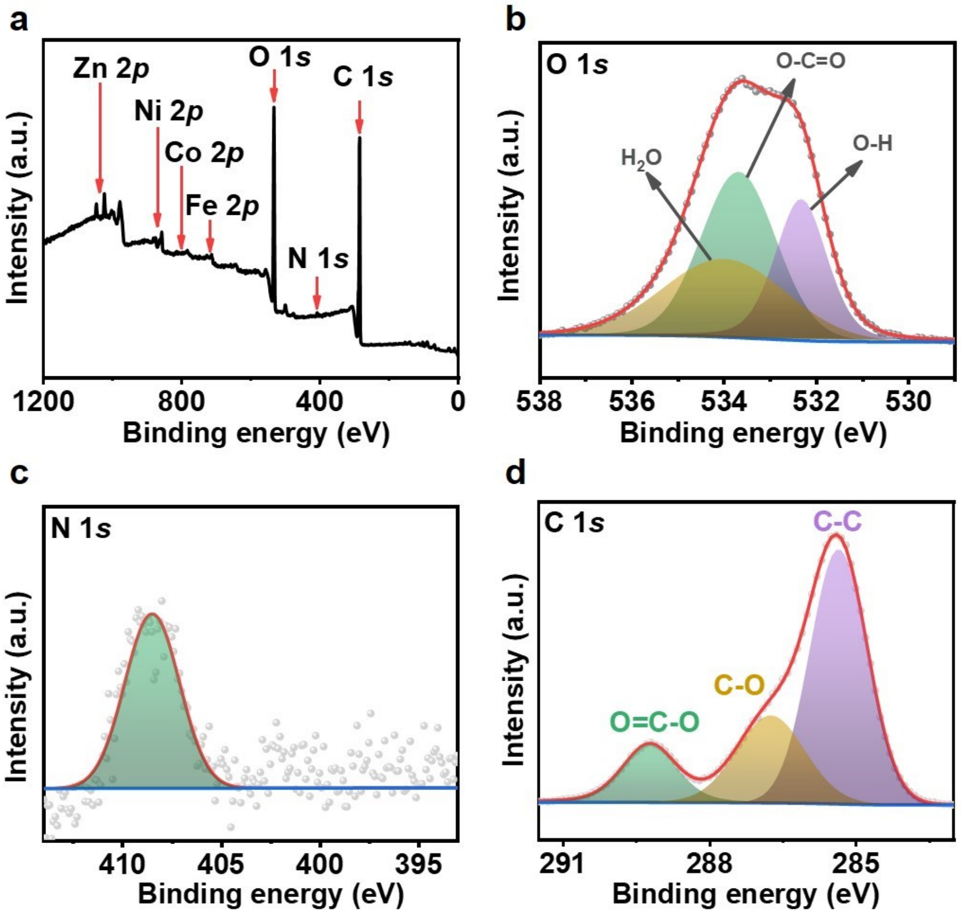

Fig. S5 XPS spectra of (a)TSH-LDH; and its high-resolution XPS spectra of (b) O, (c) N, and (d) C.

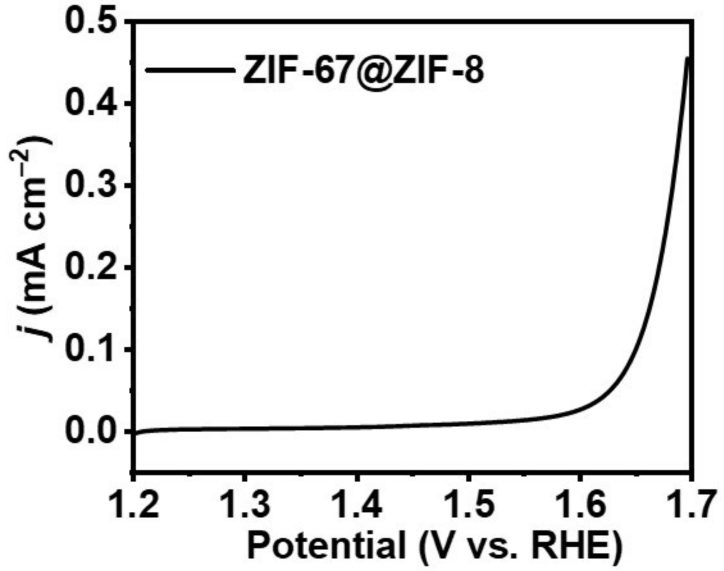

Fig. S6 Polarization curve of ZIF-67@ZIF-8.

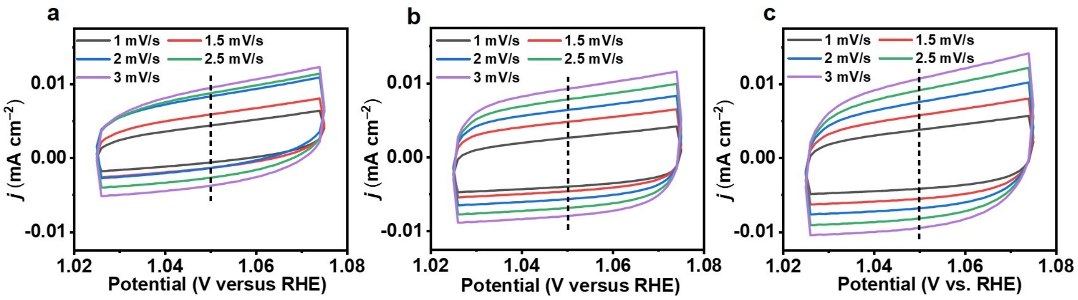

Fig. S7 The CV curves of (a) SSH-LDH, (b) DSH-LDH and (c) TSH-LDH at different scan rates.

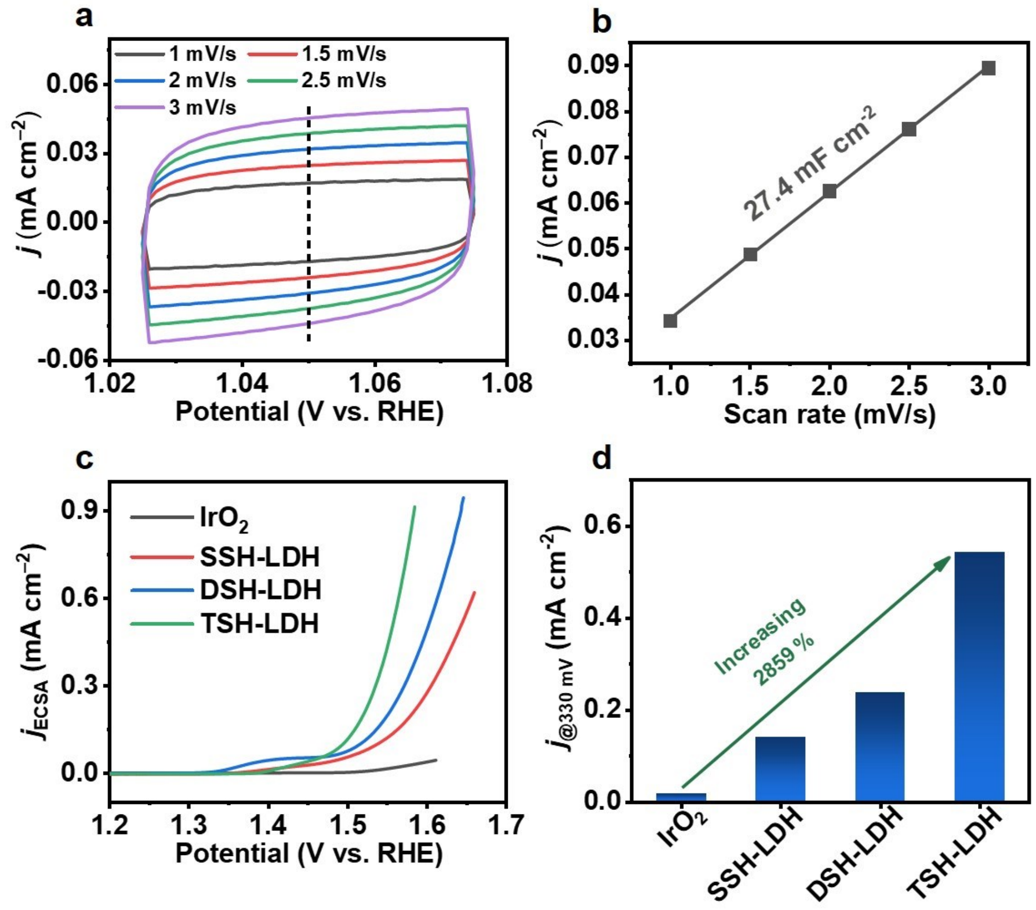

Fig. S8 The (a) CV curves and (b) C_{dl} calculation of IrO_2. (c) LSV curves and (d) current densities when at $\eta = 330$ mV after normalized by ECSA.

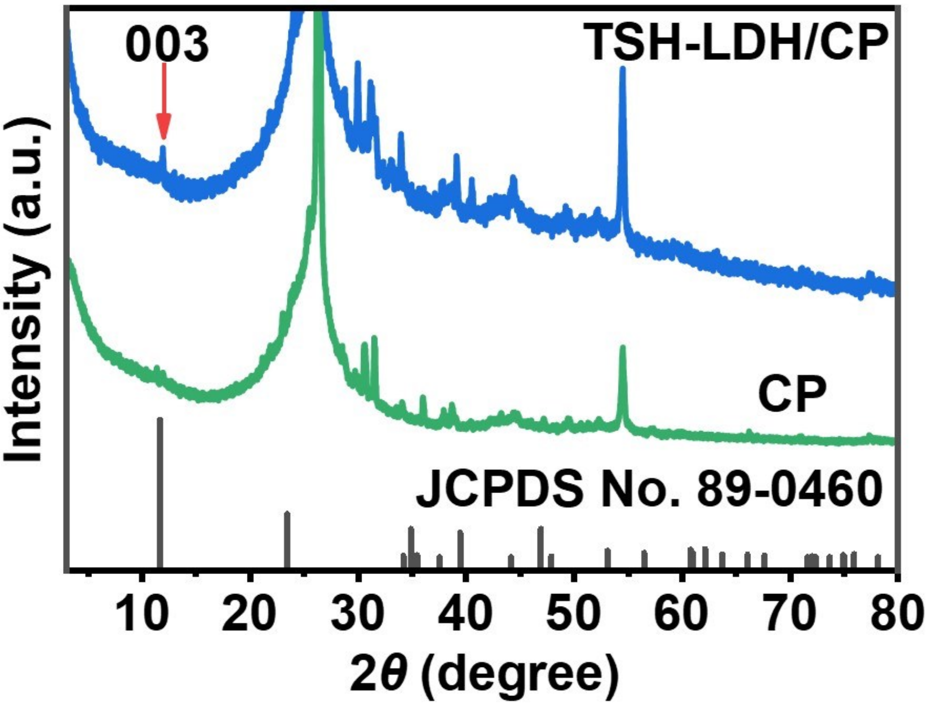

Fig. S9 XRD patterns of carbon paper (CP) and TSH-LDH/CP after the stability test.

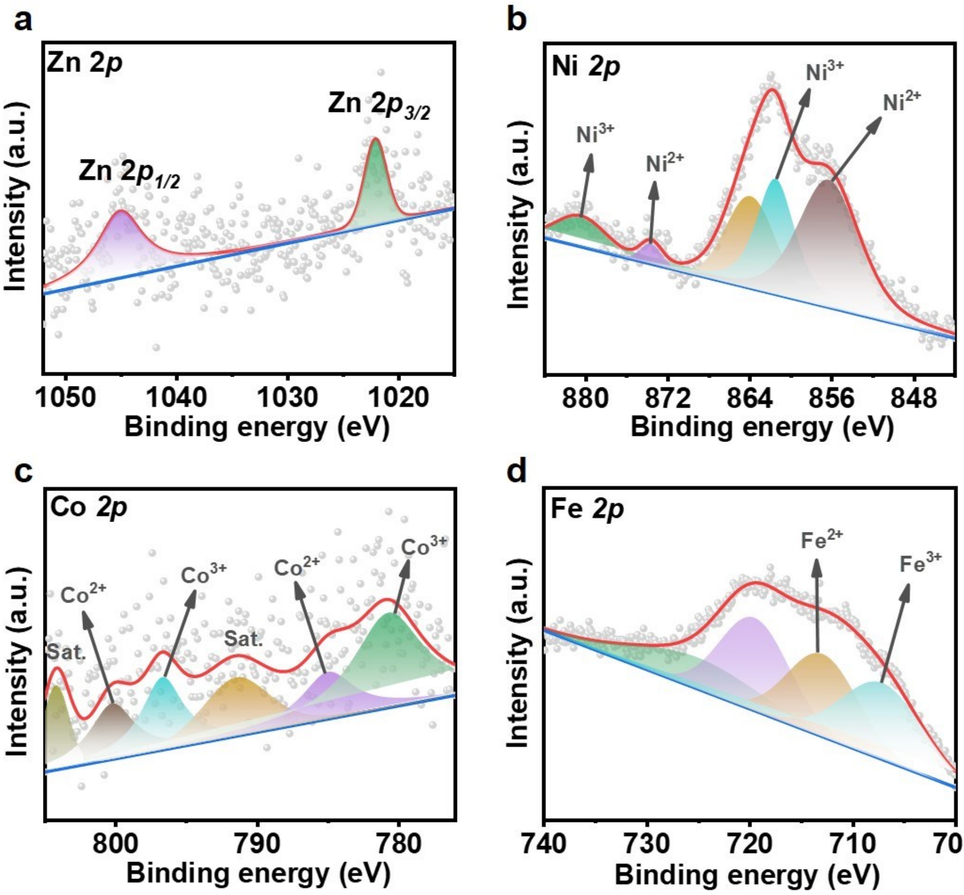

Fig. S10 High resolution XPS spectra of Zn (a), Ni (b), Co (c), Fe (d) for the TSH-LDH after the stability test.

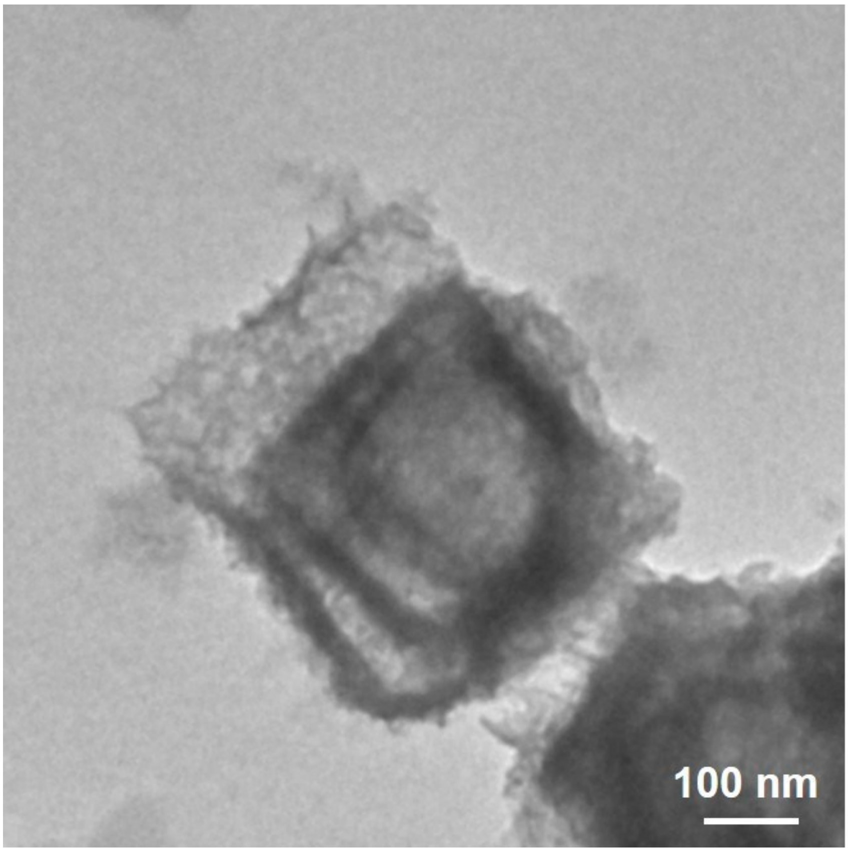

Fig. S11 TEM image of TSH-LDH after the stability test.

Table S1 The OER performance comparison of LDH related electrocatalysts.

Sample	Synthetic temperature	Electrolyte	$\eta_{10\ \mathrm{mA\ cm^{-2}}}$ (mV)	Tafel slope (mV dec^{-1})	Stability (h)	ref
NiFe-LDH NP film	120 ℃	0.1 M KOH	230	50	10	Chem. Commun. 2014, 50, 6479
NiFe-LDH	100 ℃	0.1 M KOH	270	-	-	J. Am. Chem. Soc. 2015, 137, 15090.
NiCo-LDH	160 ℃	1 M KOH	367	40	6	Nano Lett. 2015, 15, 1421
CoFe-OOH	Electro deposition	1 M KOH	300	~30	2	J. Am. Chem. Soc. 2015, 137, 3638
amorphous CoFe-H nanosheets	Electro deposition	1 M KOH	280	28	~40	Adv. Funct. Mater. 2017, 27, 1603904
NiFeV-LDH	120 ℃	1 M KOH	195 @ 20 mA cm^{-2}	42	18	Adv. Energy Mater. 2018, 8, 1703341.
NiFeCr-LDH	120 ℃	1 M KOH	225 @ 25 mA cm^{-2}	69	6	Adv. Energy Mater. 2018, 8, 1703189
Fe–Ni LDH/MOF-b2	120 ℃	1 M KOH	255	24	24	Nanoscale, 2020, 12, 14514
NiCoFe-LDH HP	Room temperature	1 M KOH	276	56	12	J. Energy Chem. 2020, 43, 104

Ni–Fe LDH DSNCs	100 ℃	1 M KOH	246 @ 20 mA cm^{-2}	71	50	Adv. Mater. 2020, 32, 1906432
MSH-LDH	Room temperature	1 M KOH	290	86.5	~60 h	This work